JACS
JOURNAL OF THE AMERICAN CHEMICAL SOCIETY
Article
pubs.acs.org/JACS

Application of the Molecular Interaction Volume Model (MIVM) to Calcium-Based Liquid Alloys of Systems Forming High-Melting Intermetallics

Sophie Poizeau and Donald R. Sadoway*

Department of Materials Science and Engineering, Massachusetts Institute of Technology, Cambridge, Massachusetts 02139-4307, United States

ABSTRACT: The thermodynamic properties of multiple liquid alloys with strong negative deviation from ideality were successfully modeled by the molecular interaction volume model (MIVM). The modeled partial Gibbs free energy of calcium in Ca−Ag, Ca−In, Ca−Pb, Ca−Sn, Ca−Tl, and Ca−Zn at 800 °C was within 1.5 kJ/mol of the existing experimental data. The partial Gibbs free energy of calcium in Ca−Bi liquid alloys at 600 °C was predicted within 1.6 kJ/mol (or 1%) by the MIVM from experimental data at 800 °C. For the first time, the MIVM was applied to a ternary system far from ideality, Ca−Sb−Pb. The partial Gibbs free energy of Ca in six Ca−Pb−Sb alloys was determined by emf measurements in a cell configured as Ca(s)|CaF_2(s)|Ca−Sb−Pb, over the temperature range of 500−830 °C. These values were 2% (or 5 kJ/mol) more negative than those predicted by the MIVM using experimental data for the Ca−Pb, Ca−Sb, and Pb−Sb binary alloys. This difference was attributed to the inability of the MIVM to account for interactions between the first nearest neighbors of Ca, Pb and Sb in the ternary Ca−Sb−Pb alloy.

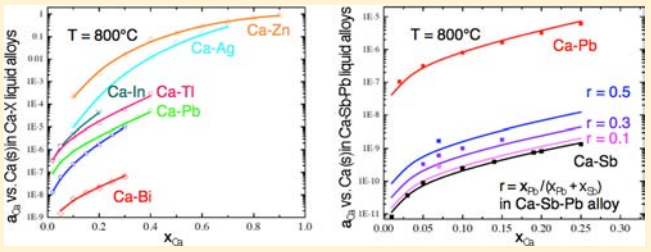

INTRODUCTION

The interest in Ca-based liquid alloys has grown with the recent developments in liquid metal batteries.[1] Compared to other candidate metals for the negative electrode in such devices, e.g., Mg,[2] Li, or Na,[3] Ca is both abundant and cheap and operates at a comparable or higher voltage for a given positive electrode.

The open circuit voltage of a Ca||X liquid metal battery, where X signifies the positive electrode, is proportional to the partial Gibbs free energy of Ca in the Ca−X alloy, $\Delta\overline{G}_{Ca}$, or the activity of Ca in Ca−X alloy, a_{Ca}, by the Nernst equation: $E = -\Delta\overline{G}_{Ca}/2F = -RT\ln(a_{Ca})/2F$. Therefore, Ca−X alloys exhibiting strong negative deviation from ideality would be the basis for high-voltage Ca−X liquid metal batteries and are of interest for this application. As can be observed with Li−Sb[4] and Na−Bi,[5] alloys with strong negative deviation from ideality usually form high-melting intermetallics.

Experimental data are available for liquid alloys of Ca−X systems forming high-melting intermetallics, namely, Ca−Ag, Ca−Bi, Ca−In, Ca−Pb, Ca−Sb, Ca−Sn, Ca−Tl, and Ca−Zn. The first goal of this study was to model these data to obtain the full theoretical discharge curve of the corresponding liquid metal batteries as a function of temperature. The second goal was to predict the thermodynamic properties of a ternary alloy, Ca−Sb−Pb, which, in turn, gives the theoretical discharge curve of a Ca||Sb−Pb liquid metal battery. The accuracy of the prediction will be assessed by comparing it to experimental data obtained in the present study.

In previous work, the MIVM was shown to be capable of modeling the thermodynamic properties of Ca−Sb liquid alloys.[6] Here, the model's utility is assessed in many more systems exhibiting strong negative deviation from ideality. As an alternative to the regular association model, which is the most common choice for systems with high-melting intermetallics, the MIVM has the advantage that its formulation does not require assumptions regarding the presence and composition of an associate and uses fewer fitting parameters (2 instead of 5). Tao[7] showed how his model can be used to predict the properties of a multicomponent system, but only in the case of nearly ideal alloys. Here, the effectiveness of the MIVM to predict the properties of a ternary alloy exhibiting a strong negative deviation from ideality was examined.

APPLICATION OF THE MIVM TO CA−X BINARY ALLOYS

MIVM Formulation. Developed by Tao,[8] the MIVM is a fluid-based model derived from statistical thermodynamics. It takes into account physical properties of the pure metals constituting the alloy, namely the molar volume, V_m, and the first coordination number, Z, in the liquid state. These two input parameters are temperature dependent.[9,10] Table 1 presents the values of these physical parameters for the metals of interest in this work.[9,10] When the temperature of interest lies below the melting point of a metal, the value of the input parameter at its melting point is adopted (e.g., Ag and Ca). However, these properties do not vary much with temperature.[9,10]

Received: February 6, 2013
Published: April 26, 2013

   dx.doi.org/10.1021/ja4013886 | J. Am. Chem. Soc. 2013, 135, 8260−8265

Table 1. Input Parameters in the MIVM

metal	T (K)	V_m (m^3/mol)[9]	Z[10]
Ag	1235	11.6	10.8
Bi	1073	22.1	9.4
Ca	1115	29.5	10.3
In	1073	17.3	10.9
Pb	1073	20.6	10.3
Sb	1073	19.3	8.62
Sn	1073	17.8	9.6
Tl	1073	19.0	10.7
Zn	1073	10.6	10.8

For the activity coefficients of i and j in a binary $i-j$ alloy, γ_i and γ_j, Tao derived new expressions which introduce two pair-potential energy interaction parameters, B_{ij} and B_{ji}.[8]

$$\ln \gamma_i = \ln\left(\frac{V_{mi}}{x_i V_{mi} + x_j V_{mj} B_{ji}}\right) + x_j\left(\frac{V_{mj}B_{ji}}{x_i V_{mi} + x_j V_{mj} B_{ji}} - \frac{V_{mi}B_{ij}}{x_j V_{mj} + x_i V_{mi} B_{ij}}\right) - \frac{x_j^2}{2}\left(\frac{Z_i B_{ji}^2 \ln B_{ji}}{(x_i + x_j B_{ji})^2} + \frac{Z_j B_{ij} \ln B_{ij}}{(x_j + x_i B_{ij})^2}\right) \quad (1)$$

A similar expression describes how γ_j varies with composition.

Determination of the Interaction Coefficients. To determine the value of B_{CaX} and B_{XCa} in Ca–X alloys, the activity of Ca in Ca–X alloys, a_{Ca}, was fitted with the MIVM expression. In his work on near-ideal liquid alloys,[8] Tao minimized the error in a_{Ca}. Here, the activities, which span several orders of magnitude, were obtained by emf measurements. Since $\Delta\bar{G}_{Ca} = RT \ln(a_{Ca})$, the error in $\ln(a_{Ca})$, as opposed to a_{Ca}, was minimized via a nonlinear least-squares analysis, using an iterative method developed on MuPAD, the numerical solver of MATLAB. This iterative method optimizes the interaction parameters by keeping one constant and optimizing the other one and then keeping the other constant and optimizing the former. The norm 2 of the error vector, $\mathrm{err} = (\sum_{i=1}^{n}(\ln(a_{Ca,exp}) - \ln(a_{Ca,MIVM}))^2)^{1/2}/n$, with n the number of experimental data points, was the parameter minimized through the optimization (see Figure 1).

To ensure that the solution for the interaction coefficients did not depend on the choice of starting values in the optimization program, $\mathrm{err}(B_{CaX},B_{XCa})$ was plotted in 3D. As can be seen in Figure 1 in the representative case of Ca–Sn, there was only one minimum in this function, and the coordinates of this minimum were identical to the values found via the optimization algorithm.

Results at 800 °C. Experimental data for all the Ca–X alloys of interest (Ca–Ag, Ca–Bi, Ca–In, Ca–Pb, Ca–Sn, Ca–Tl, and Ca–Zn) were available from the extensive studies done at 800 °C by Delcet et al.[11−13] at Brookhaven National Laboratory, who obtained all these data by coulometric titration vs a Ca–Bi (l) reference electrode through a single crystal CaF_2 electrolyte. In the case of Ca–Bi, these data were consistent with the emf measurements of Kim et al.,[14] taken vs a Ca(s) reference electrode using a sintered CaF_2 electrolyte.

The modeled values are compared to the experimental data in Figure 2. The values found for B_{CaX} and B_{XCa} at 800 °C are listed in Table 2, with the number of data points used in the fit. To evaluate the goodness of fit, the average error in the partial Gibbs free energy of Ca is also indicated. The error is defined as

$$\Delta\bar{G}_{Ca,MIVM} - \Delta\bar{G}_{Ca,exp} = RT \ln \frac{a_{Ca,MIVM}}{a_{Ca,exp}} \quad (2)$$

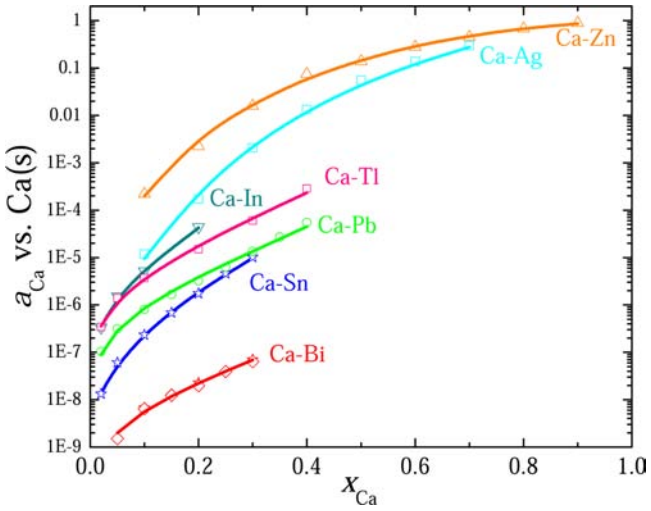

Figure 2. Ca activity vs Ca concentration in Ca–X liquid alloys at 800 °C, experimental data represented by the symbols (Ca–Zn from ref 13, Ca–Ag and Ca–In from ref 12, Ca–Pb and Ca–Tl from ref 11, Ca–Bi from ref 11 (★) and ref 14 (□)). Solid lines represent a_{Ca} modeled herein by the MIVM.

Table 2. Values Found for the Pair Potential Interaction Parameters in Ca–X Liquid Alloys at 800 °C, with Number of Data Points Used in the Optimization Algorithm, and Error in the Modeled Partial Gibbs Free Energy of Calcium

X	B_{CaX}	B_{XCa}	no. of data points	average $\Delta\bar{G}_{Ca}$ error (kJ/mol)
Ag	1.89	1.87	7	±1.5
Bi	1.15	14.26	10	±0.9
In	1.39	3.65	4	±0.6
Pb	1.15	6.34	9	±1.1
Sn	1.46	5.94	7	±0.4
Tl	1.17	4.86	6	±1.1
Zn	1.73	1.25	9	±0.7

Temperature Dependence. According to Tao's model, the temperature dependence of B_{ji} is given by $B_{ji} = \exp(-(\varepsilon_{ji} - \varepsilon_{ii})/kT)$,

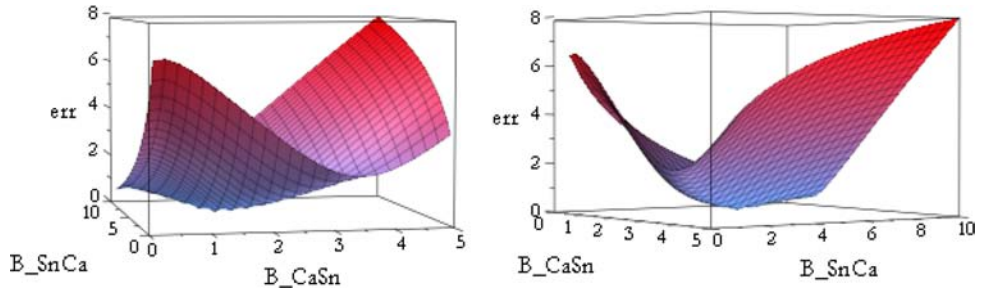

Figure 1. Representative case of err as a function of B_{CaSn} and B_{SnCa} in the case of Ca–Sn liquid alloys at 800 °C (minimum obtained for B_{CaSn} = 1.46 and B_{SnCa} = 5.94).

dx.doi.org/10.1021/ja4013886 | J. Am. Chem. Soc. 2013, 135, 8260−8265

with ε_{ji} the pair potential energy of a central i atom and its first nearest neighbor j.[8] The temperature dependence of B_{ij} is defined similarly. Assuming a constant $\varepsilon_{ji} - \varepsilon_{ii}$, one can predict the values of the interaction coefficients of Ca−X liquid alloys at different temperatures. The temperature dependence was verified for alloys exhibiting thermodynamic properties with strong negative deviation from ideality in the case of Ca−Sb.[6]

Of all the Ca−X alloys of interest here, experimental data were available at $T \neq 800$ °C for Ca−Bi and Ca−Pb. Kim et al. provided data for an array of temperatures between 600 and 800 °C.[14] In the case of Ca−Pb, additional experimental data at 900 °C were collected by Fray et al.[15] by coulometric titration vs a Ca (l) reference electrode through solid calcium magnetoplumbite ($CaCO_3$−$MgCO_3$−α-Al_2O_3 mixture).

Knowing how the interaction coefficients depend on temperature, one can predict the activity of Ca in Ca−X alloys at other temperatures using the $\varepsilon_{ji} - \varepsilon_{ii}$ obtained at 800 °C: at 600 °C in the case of Ca−Bi and at 900 °C in the case of Ca−Pb. In the case of Ca−Bi, the predicted values match the experimental data, while this is not the case for Ca−Pb (Figure 3, Table 3). The inconsistency between the data of Delcet et al.[11] and Fray et al.[15] was already reported in the literature, by both Fray et al.[15] and Cartigny et al.[16]

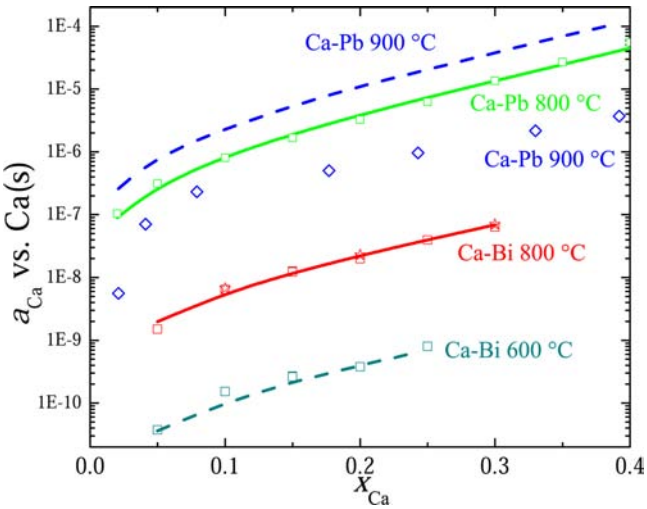

Figure 3. Ca activity vs Ca concentration in Ca−Bi and Ca−Pb liquid alloys at different temperatures. Experimental data represented by the symbols (Ca−Bi from refs 11 (★) and 14 (□), Ca−Pb from refs 11 (□) and 15 (◇)), data modeled herein by the MIVM represented by the solid lines, data predicted herein by the MIVM, from the data at 800 °C, represented by the dash lines.

Table 3. Values for the Pair Potential Interaction Parameters in Ca−Bi and Ca−Pb Liquid Alloys Calculated from Their Values at 800 °C and Error in the Modeled Partial Gibbs Free Energy of Calcium

X	T (K)	B_{CaX}	B_{XCa}	average $\Delta\bar{G}_{Ca}$ error (kJ/mol)
Bi	873	1.19	26.21	±1.6
Pb	1173	1.13	5.41	28

APPLICATION OF THE MIVM TO CA−SB−PB TERNARY LIQUID ALLOYS

Prediction. Tao derived the variation of activity with concentration for each component of an i−j−k ternary alloy[8] by assuming that the energy of a j atom next to a central i atom is the same in the presence or absence of a k atom next to the i atom.

Before the properties of Ca−Sb−Pb liquid alloys can be predicted, the properties of Ca−Sb, Ca−Pb and Pb−Sb liquid alloys must be optimized using the MIVM. The properties of Ca−Sb and Ca−Pb have already been optimized in ref 6 and in this paper, respectively. The experimental data used in the optimization of the Pb−Sb system were obtained by Sebkova et al.[17] by emf measurements using a molten salt electrolyte of $PbCl_2$ in KCl−NaCl (eutectic), where the emf signal of the Pb−Sb alloy was recorded vs Pb (l). Sebkova reported the emf of Pb−Sb alloys in the $0.216 < x_{Pb} < 0.914$ range at 700, 750, and 800 °C. The properties both at 700 and 800 °C were used to check the accuracy of the MIVM regarding the temperature dependence and are plotted in Figure 4. The average error

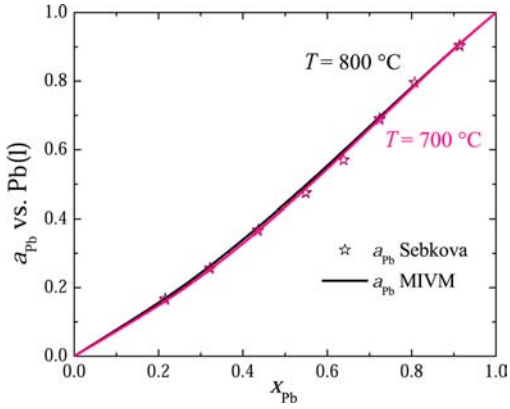

Figure 4. Pb activity vs Pb concentration in Sb−Pb liquid alloys at 700 and 800 °C, modeled by the MIVM and measured by Sebkova.[17]

obtained between the measured emf and the modeled value was 0.8 mV at both temperatures. This corresponds to an error in the partial Gibbs free energy of Pb of ±0.1 kJ/mol.

Based on the Tao's formula, the activity coefficient of Ca in Ca−Sb−Pb liquid alloys can be expressed as:

$$\ln \gamma_{Ca} = 1 + \ln \frac{V_{mCa}}{x_{Ca}V_{mCa} + x_{Sb}V_{mSb}B_{SbCa} + x_{Pb}V_{mPb}B_{PbCa}} - \frac{x_{Ca}V_{mCa}}{x_{Ca}V_{mCa} + x_{Sb}V_{mSb}B_{SbCa} + x_{Pb}V_{mPb}B_{PbCa}} - \frac{x_{Sb}V_{mCa}B_{CaSb}}{x_{Ca}V_{mCa}B_{CaSb} + x_{Sb}V_{mSb} + x_{Pb}V_{mPb}B_{PbSb}} - \frac{x_{Pb}V_{mCa}}{x_{Ca}V_{mCa}B_{CaPb} + x_{Sb}V_{mSb}B_{SbPb} + x_{Pb}V_{mPb}} - 0.5\left(Z_{Ca} \times \frac{(x_{Sb}B_{SbCa} + x_{Pb}B_{PbCa})(x_{Sb}B_{SbCa}\ln B_{SbCa} + x_{Pb}B_{PbCa}\ln B_{PbCa})}{(x_{Ca} + x_{Sb}B_{SbCa} + x_{Pb}B_{PbCa})^2} + \frac{Z_{Sb}x_{Sb}B_{CaSb}((x_{Sb} + x_{Pb}B_{PbSb})\ln B_{CaSb} - x_{Pb}B_{PbSb}\ln B_{PbSb})}{(x_{Ca}B_{CaSb} + x_{Sb} + x_{Pb}B_{PbSb})^2} + \frac{Z_{Pb}x_{Pb}B_{CaPb}((x_{Sb}B_{SbPb} + x_{Pb})\ln B_{CaPb} - x_{Sb}B_{SbPb}\ln B_{SbPb})}{(x_{Ca}B_{CaPb} + x_{Sb}B_{SbPb} + x_{Pb})^2}\right) \quad (3)$$

The temperature-independent pair potential energies in Sb−Pb alloys are reported in Table 4 along with those calculated for Ca−Sb and Ca−Pb. These parameters, along with the properties of the pure metals from Table 1, are all that is needed to predict the activity of Ca in Ca−Sb−Pb ternary liquid alloys.

dx.doi.org/10.1021/ja4013886 | J. Am. Chem. Soc. 2013, 135, 8260−8265

Table 4. Temperature-Independent Pair Potential Energies; $\varepsilon_{ij} - \varepsilon_{jj} = -kT \ln B_{ij}$ (eV)

	i		
j	Ca	Sb	Pb
Ca	0	−0.294	−0.171
Sb	−0.014	0	−0.016
Pb	−0.013	0.013	0

Comparison with Experimental Measurements. To assess the accuracy of the MIVM to predict the partial thermodynamic properties of mixing of Ca−Sb−Pb liquid alloys, emfs of 6 Ca−Sb−Pb alloys in Ca(s)|CaF_2|Ca−Sb−Pb cells were measured, at fixed concentrations, over the temperature range of 500−830 °C Figure 5. The same emf setup was used as in the case of Ca−Sb alloys.[6] The advantage of such a method is that slope changes in the emf allow the identification of first-order phase transitions (e.g., from l to s+l phase).[6] Since the MIVM expression for the activity coefficient of Ca is valid only in a fully liquid alloy, it was important to be able to choose an experimental approach that would allow this identification.

The overall cell reaction is the alloying of Ca in Pb−Sb according to the following half reactions:

$$\text{reference electrode(RE): } Ca_{(s)} = Ca^{2+} + 2e^-$$

$$\text{working electrode(WE): } Ca^{2+} + 2e^- = Ca_{\text{inPb}-\text{Sb}}$$

The emf E measured between the reference and working electrodes can be expressed by the Nernst equation:

$$E_{RE} = E^0_{Ca} + \frac{RT}{2F}\ln a_{Ca^{2+}} \quad (4)$$

$$E_{WE} = E^0_{Ca} + \frac{RT}{2F}\ln\left(\frac{a_{Ca^{2+}}}{a_{Ca}}\right) \quad (5)$$

$$E = E_{WE} - E_{RE} = -\frac{RT}{2F}\ln a_{Ca} \quad (6)$$

where E^0_{Ca} is the standard potential of pure calcium at T, absolute temperature, and R and F are the gas and Faraday constants, respectively. The activity of Ca^{2+} in the electrolyte, $a_{Ca^{2+}}$, is the same in eqs 4 and 5. The activity of Ca in the Ca−Sb−Pb alloy, a_{Ca}, is the only unknown and can be directly calculated from the emf. The standard state is pure calcium in its most stable state at any given temperature.

The predicted and the measured emfs for Ca(s)|CaF_2|Ca−Sb−Pb (l) cells are compared in Table 5 at 700 and 800 °C. Figure 6 presents how the activity of Ca varies with the Ca concentration, x_{Ca}, in the liquid positive electrode of a Ca||Pb−Sb (ratio $r = x_{Pb}/(x_{Sb} + x_{Pb})$) liquid metal battery at 800 °C. The theoretical discharge curve of such a battery is related to a_{Ca} via the Nernst equation $E = -RT\ln(a_{Ca})/2F$. The experimental values of the activity of Ca, measured by emf in the corresponding Ca−Sb−Pb liquid alloys, are presented in Figure 6 for comparison with the MIVM prediction.

The predicted emf is on average 24 mV higher than the measured emf, which represents only a 2% error. This corresponds to an average error of 5 kJ/mol in the partial Gibbs free energy of Ca, while the error was 1 kJ/mol on average in the case of Ca−Pb and Ca−Sb. This suggests that on a first pass the strength of the interaction between the atoms and their respective first nearest neighbors is similar in the binary and ternary alloys, and the MIVM predicts the activity of Ca in a Ca−Sb−Pb alloy rather well. However, the increase in error suggests that the strength of these interactions is affected.

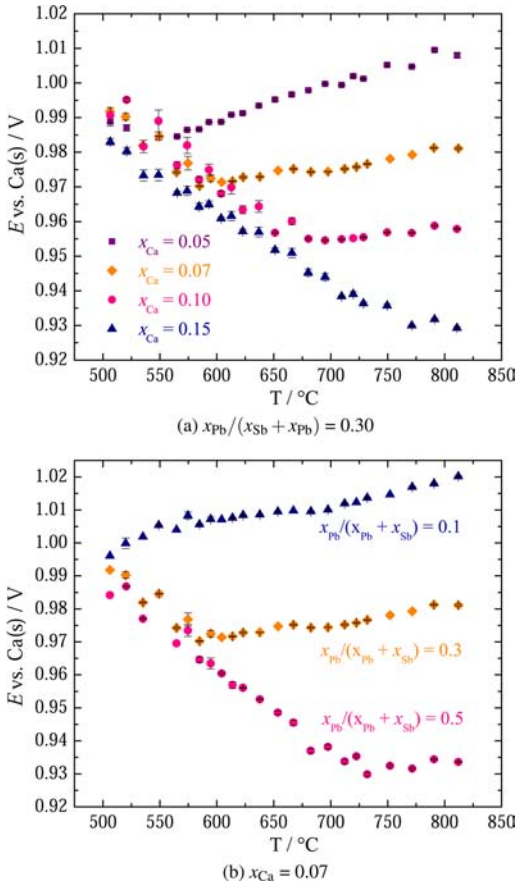

Figure 5. Measured values of emf vs temperature in Ca(s)|CaF_2|Ca−Sb−Pb cells between 500 and 830 °C.

Table 5. Comparison between the emf Measured in Ca(s)|CaF_2|Ca−Pb−Sb (l) and Predicted by the MIVM, Using the Interaction Coefficients Obtained from the Modeling of the Binary Systems

x_{Ca}	$(x_{Pb}/(x_{Sb} + x_{Pb}))$	T (°C)	emf predicted (V)	emf measured (V)	$\Delta\bar{G}_{Ca}$ error (kJ/mol)
0.05	0.30	700	1.022	1.000	−4
		800	1.029	1.009	−4
0.07	0.30	700	1.002	0.974	−5
		800	1.007	0.981	−5
0.07	0.10	700	1.033	1.007	−5
		800	1.041	1.017	−5
0.07	0.50	800	0.962	0.930	−5
0.10	0.30	700	0.978	0.955	−4
		800	0.981	0.958	−4
0.15	0.30	800	0.946	0.930	−3

Interpretation of the Results. In an $i-j-k$ ternary alloy, the MIVM does not account for the effect that $j-k$ interactions may have on the strengths of $i-j$ and $i-k$ interactions, changing them from their values in the respective binary alloys. In spite of this, Tao did not notice any increase in error when predicting the activity of the components in a ternary alloy using the interaction coefficients from the binary alloys in the case of near-ideal ternary alloys.[7] Figure 7 shows the environment of each atom in Ca−Pb−Sb liquid alloys, and it appears that the environments of Pb and Sb are quite different from the environment of Ca. When Pb or Sb is the central atom, $\delta_{ij} = \varepsilon_{ij} - \varepsilon_{jj}$, with j the central atom and

dx.doi.org/10.1021/ja4013886 | J. Am. Chem. Soc. 2013, 135, 8260−8265

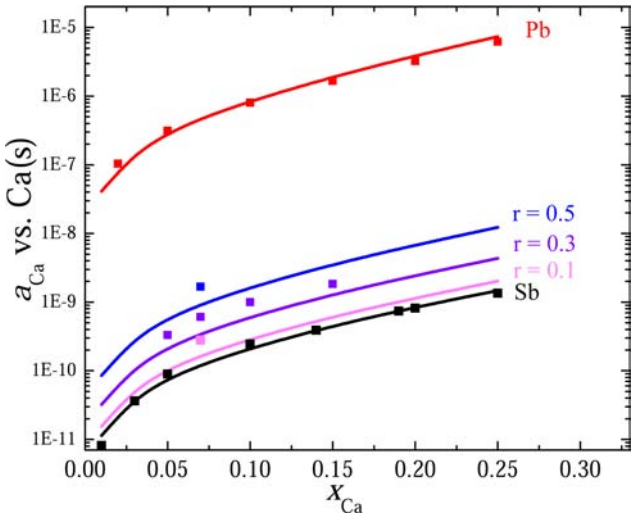

Figure 6. Ca activity vs Ca concentration in Ca−Sb−Pb liquid alloys at 800 °C for fixed $r = x_{Pb}/(x_{Sb} + x_{Pb})$ ratios. The lines represent the data predicted by the MIVM using the interaction coefficients obtained from the modeling of the binary alloys. The squares represent the experimental data obtained by emf measurements. The data for Ca−Pb is from Delcet,[11] the data for Ca−Sb is from ref 6, and the other data points were obtained in this work.

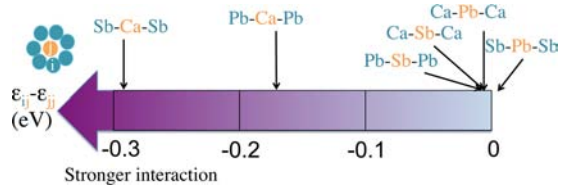

Figure 7. Environment of each atom in Ca−Pb−Sb liquid alloys; $\varepsilon_{ij} - \varepsilon_{jj}$, with j central atom (in orange) and i first nearest neighbor (in green) determined from MIVM modeling of the i−j binary alloys.

i the type of peripheral atom, is close to 0. This means that the pair potential energies ε_{ij} between i = Ca, Pb, or Sb, first nearest neighbors, and their respective central atoms, j = Pb or Sb, have comparable values. This is similar to what happens in the near-ideal alloys considered by Tao. However, in the case of the environment of Ca, we observe that δ_{SbCa} and δ_{PbCa} are quite different, as compared to what is calculated in the binary alloys Sb−Ca and Pb−Ca. This is inconsistent with the idea that Pb and Sb are very similar atoms forming an alloy with thermodynamic properties close to ideality and mixing randomly. Therefore, the interaction between Pb and Sb, when both are present in the ternary alloy, is probably affecting the strength of the interaction between Ca and its nearest neighbors, Pb and Sb, forcing the difference between δ_{SbCa} and δ_{PbCa} to shrink.

To test this hypothesis, δ_{SbCa} and δ_{PbCa} were fitted to the experimental data at 700 and 800 °C, while the values for δ_{iPb} and δ_{iSb} obtained from the binary fitting were retained. Three out of the six Ca−Sb−Pb alloys, which correspond to $r = 0.3$, with x_{Ca} = 0.05, 0.07 and 0.10, were used for the fitting. As the analysis suggested, δ_{SbCa} and δ_{PbCa} are closer in a Ca−Sb−Pb alloy than in the respective Ca−X binary alloys: $\delta_{SbCa} = -0.285$ eV and $\delta_{SbCa} = -0.198$ eV. Using these new values, the difference was ±2 mV between the modeled and the experimental emf or ±0.4 kJ/mol for $\Delta\bar{G}_{Ca}$ for the 3 alloys concerned.

With the new values, the Ca activity in Ca−Sb−Pb alloys was predicted for the other alloys as well, which have compositions outside the range used for the fitting (Table 6). In Figure 8, the

Table 6. Comparison between the emf Measured in Ca(s)|CaF_2|Ca−Pb−Sb (l) and Predicted by the MIVM, Using the Corrected Interaction Coefficients

x_{Ca}	$(x_{Pb}/(x_{Sb} + x_{Pb}))$	T (°C)	emf predicted (V)	emf measured (V)	$\Delta\bar{G}_{Ca}$ error (kJ/mol)
0.05	0.30	700	0.998	1.000	0.4
		800	1.007	1.009	0.5
0.07	0.30	700	0.978	0.974	−0.6
		800	0.984	0.981	−0.7
0.07	0.10	700	1.007	1.007	−0.002
		800	1.016	1.017	−0.2
0.07	0.50	800	0.945	0.934	−2
0.10	0.30	700	0.954	0.955	0.2
		800	0.958	0.958	0.03
0.15	0.30	800	0.923	0.930	−1

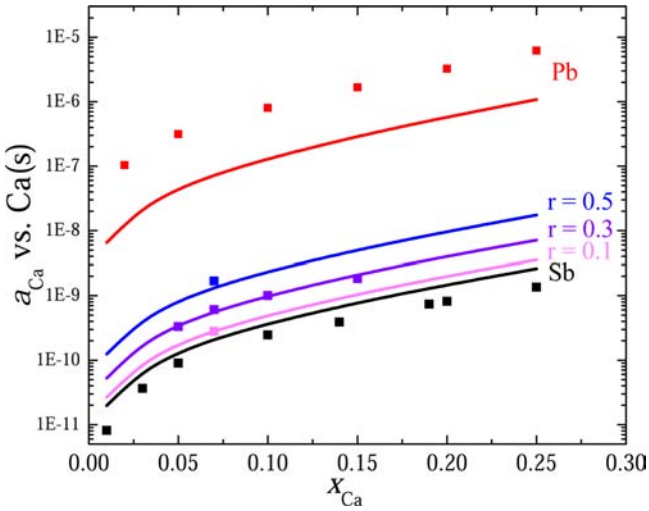

Figure 8. Ca activity vs Ca concentration in Ca−Sb−Pb liquid alloys at 800 °C for fixed $r = x_{Pb}/(x_{Sb} + x_{Pb})$ ratios. The lines represent the data predicted by the MIVM after correction of the coefficients corresponding to the first nearest neighbors of Ca, and the squares represent the experimental data measured by emf. The data for Ca−Pb is from Delcet,[11] the data for Ca−Sb is from ref 6, and the other data points were obtained in this work.

measured and predicted a_{Ca} at 800 °C are compared for all the different Ca−Sb−Pb alloys of interest. On average, the error between the experimental and predicted emfs for these 3 other alloys is ±6 mV, or 0.6% of the emf measured. This corresponds to an average error of 1 kJ/mol in $\Delta\bar{G}_{Ca}$.

As seen in Figure 8, the activity of Ca in the binary alloys Ca−Sb and Ca−Pb is not well represented when calculated using the interaction coefficients obtained from the modeling of the ternary alloy. Therefore, this suggests that the energy coefficients are indeed altered in the ternary alloy. The interaction between the first nearest neighbors of Ca, namely Pb and Sb, can be taken into account by examination of its impact on the interaction between the Ca and its first nearest neighbors, and correcting the corresponding coefficients accordingly.

■ CONCLUSION

The MIVM was applied successfully to many Ca-based alloys of systems with high-melting intermetallics, namely Ca−Ag, Ca−Bi, Ca−In, Ca−Pb, Ca−Sn, Ca−Tl, and Ca−Zn. The temperature dependence of the interaction coefficients was verified in

dx.doi.org/10.1021/ja4013886 | J. Am. Chem. Soc. 2013, 135, 8260−8265

the case of Ca−Bi alloys over the temperature range of 500−830 °C. In addition, the MIVM was used to predict the activity of a component, Ca, in a ternary system, Ca−Sb−Pb, whose thermodynamic properties exhibit strongly negative deviation from ideality, which has not been demonstrated before to the authors' knowledge. The prediction was good (2% difference with experimental measurements), but unlike alloys of similar elements,[7] the interaction between Sb and Pb atoms around Ca atoms was not completely negligible.

The MIVM allows one to predict, from partial experimental data at one temperature, the activity of Ca—and therefore the theoretical discharge curve of Ca||X liquid metal batteries—at different temperatures, without assuming the presence of an associate species. This makes MIVM the model of choice in the study of liquid metal batteries. Indeed, using the MIVM, one can predict at different temperatures the theoretical discharge curve of different A||B liquid metal batteries from thermodynamic data obtained at one temperature. Therefore, the maximal energy that can be stored by the liquid metal battery can be calculated before running any battery measurement, allowing one to assess which A||B liquid metal batteries are worth testing. Knowing the theoretical discharge curve of the battery, the performance of the battery can then be evaluated by comparing it to the actual discharge curve.

The prediction of the activity in the case of a ternary alloy is also particularly useful for anticipating how the addition of an element impacts the theoretical discharge curve of the battery. Further study of the ternary phase diagrams and evaluation of the maximum solubility of Ca in the ternary alloy would however be necessary to fully assess how the addition of this element affects the capacity of such Ca-based liquid metal batteries.

AUTHOR INFORMATION

Corresponding Author

dsadoway@mit.edu

Notes

The authors declare no competing financial interest.

ACKNOWLEDGMENTS

The authors acknowledge J. M. Newhouse, Dr. H. Kim, Dr. T. Ouchi, and Dr. B. H. Chung from the Sadoway group for their fruitful discussions and advice, TOTAL S.A., and the US Department of Energy, Advanced Research Projects Agency - Energy (award no. DE-AR000047) for their financial support.

REFERENCES

(1) Kim, H.; Boysen, D.; Newhouse, J. M.; Spatocco, B. L.; Chung, B.; Burke, P. J.; Bradwell, D. J.; Jiang, K.; Tomaszowska, A. A.; Wang, K.; Wei, W.; Ortiz, L.; Barriga, S. A.; Poizeau, S.; Sadoway, D. R. *Chem. Rev.* **2013**, *113*, 2075−2099.

(2) Bradwell, D. J.; Kim, H.; Sirk, A. H. C.; Sadoway, D. R. *J. Am. Chem. Soc.* **2012**, *134*, 1895−1897.

(3) Cairns, E.; Shimotake, H. *Science* **1969**, *164*, 1347−1355.

(4) Weppner, W.; Huggins, R. *J. Electrochem. Soc.* **1978**, *125*, 71−74.

(5) Iwase, M.; Sugino, S.; Ichise, E. *High Temp. Mater. Proc.* **1984**, *6*, 143−153.

(6) Poizeau, S.; Kim, H.; Newhouse, J. M.; Spatocco, B. L.; Sadoway, D. R. *Electrochim. Acta* **2012**, *76*, 8−15.

(7) Tao, D. P. *Metall. Mater. Trans. B* **2001**, *32*, 1205−1211.

(8) Tao, D. P. *Thermochim. Acta* **2000**, *363*, 105−113.

(9) Iida, T.; Guthrie, R. I. *The physical properties of liquid metals*; Clarendon Press: Oxford, 1988.

(10) Tao, D. P. *Metall. Mater. Trans. A* **2005**, *36A*, 3495−3497.

(11) Delcet, J.; Delgado-Brune, A.; Egan, J. Coulometric titrations using CaF_2 and BaF_2 solid electrolytes to study alloy phases. 26264. *Brookhaven National Laboratory*, 1979; pp 1−12.

(12) Delcet, J.; Egan, J. *J. Less-Common Met.* **1978**, *59*, 229−36.

(13) Delcet, J.; Egan, J. *Metall. Trans. B* **1978**, *9B*, 728−729.

(14) Kim, H.; Boysen, D.; Bradwell, D. J.; Chung, B.; Jiang, K.; Tomaszowska, A. A.; Wang, K.; Wei, W.; Sadoway, D. R. *Electrochim. Acta* **2012**, *60*, 154−162.

(15) Fray, D.; Kumar, R. *Scand. J. Metall.* **1993**, *22*, 266−270.

(16) Cartigny, Y.; Fiorani, J.; Maitre, A.; Vilasi, M. *Thermochim. Acta* **2004**, *414*, 197−202.

(17) Sebkova, J.; Beranek, M. *Kovove Mater.* **1979**, *17*, 393−403.